Neuroendocrinology Letters Volume 43 No. 7-8 2022
ISSN: 0172-780X; ISSN-L: 0172-780X; Electronic/Online ISSN: 2354-4716
Web of Knowledge / Web of Science: Neuroendocrinol Lett
Pub Med / Medline: Neuro Endocrinol Lett

ORIGINAL ARTICLE

Evaluating thermosensitive chitosan/β-glycerophosphate sodium and fibroblast embolization for the treatment of cerebral arteriovenous malformation in a porcine model

Xianbin Ning[1], Changfu Zhao[1], Junyi Zhao[1], Jinfeng Pang[1]

1 Department of Neurosurgery, the Affiliated Hospital of Beihua University, Jilin 132011, China.

Correspondence to: Jinfeng Pang, Professor
Department of Neurosurgery, The Affiliated Hospital of Beihua University, Jilin 132011, China.
TEL: +86 18943209366, FAX: +86 0432 62166001, E-MAIL: cnjinfengpang@126.com

Submitted: 2022-02-26 Accepted: 2022-12-28 Published online: 2022-12-28

Key words: **Chitosan/β-glycerophosphate sodium; Fibroblasts; Skull base vascular network; Intervention; Embolization; Cerebral arteriovenous malformation**

Neuroendocrinol Lett 2022; **43**(7-8):385–392 **PMID:** 36720127 NEL437822A04

Abstract

OBJECTIVE: To evaluate the feasibility of non-sticky thermosensitive liquid embolic material chitosan/β-glycerophosphate sodium (C/GP) and fibroblast embolization in rete mirabile (REM) for preparing the model of cerebral arteriovenous malformation (cAVM); to study the method of microcatheter injection of C/GP-gel system; and to observe the embolization effect and histological changes of REM.

METHODS: A total of 26 domestic pigs were grouped and prepared designed models, followed by different treatment methods using C/GP. C/GP embolization of the REM were performed. The brain samples were obtained after week 6's angiography and finally, subjected to H&E staining for histological examination.

RESULTS: In 26 pig models, 25 pigs were successfully modeled, and 1 pig had convulsions and died during the modeling process. After embolization, angiography showed that the embolized REM was no longer developed while there was no adhesion between the tip of the microcatheter and the embolization agent. No recanalization was found in week 2 and week 6's angiography. Histological examination: the hydrogel was uniformly dispersed in REM, and REM was completely embolized. The texture was hard. REM was filled by gel and fibroblasts, the intima of the wall was clearly visible, and the smooth muscle layer was intact. No exfoliation and necrosis of the vessel wall were observed, and no inflammatory reaction was observed around the blood vessel.

CONCLUSIONS: Our study provided sufficient evidence to suggest that C/GP may be a novel liquid embolic material for the endovascular treatment of cAVM. C/GP and fibroblasts can be used in the embolization of cAVM and may have broad application as an ideal embolization material for the treatment of cAVM.

Abbreviations:

AA	- arteriaanastomotica
ANOVA	- analysis of variance
AP	- ascending pharyngeal artery
cAVM	- cerebral arteriovenous malformation
CCA	- common carotid artery
C/GP	- chitosan/β-glycerophosphate sodium
CVA	- coronary venous angiography
DSA	- digital subtraction angiographic
DMEM	- Dulbecco's modified Eagle medium
H&E	- hematoxylin and eosin
IJV	- internal jugular vein
NBCA	- n-Butyl cyanide propionate
REM	- rete mirabile
RA	- ramusanastomoticus
US FDA	- US Food and Drug Administration

INTRODUCTION

Cerebral arteriovenous malformation (cAVM) is the primary cause of intracranial hemorrhage and epilepsy in young and middle-aged people and poses a serious threat to people's quality of life and longevity (Chen *et al.* 2020). cAVMs may be treated via microsurgery, radiosurgery, endovascular surgery or a combination of these modalities (Lopes *et al.* 2016), with endovascular embolization becoming an increasingly popular strategy for treating cAVM due to its minimally invasive nature. Hypertension, SM grade, cAVM size, malformed vessel location, venous drainage and the choice of embolization material are all linked to therapeutic effect (Chen *et al.* 2017). The ideal cAVM embolization material should meet some or all of the following criteria (Massoud *et al.* 2000; Murayama *et al.* 1998) 1) the material should be liquid and easy to control with good dispersion properties; 2) users should ensure sufficient injection time; 3) the embolization effect should be permanent and 3) non-toxic. In recent years, non-stick fluid embolic materials have become an ideal embolic material and have been extensively evaluated in endovascular treatment applications (Jabbour *et al.* 2009).

Given these criteria, this study used chitosan/β-glycerophosphate sodium (C/GP) as the basic material (Wang *et al.* 2011), which is liquid at room temperature, forms a hydrogel at a temperature of 37.0 °C (body temperature), and has a PH value within the human physiological range (Ning *et al.* 2015). These two non-stick thermosensitive materials are safe and non-toxic and can be applied in the embolization of cAVMs, but they experience a high degradation rate and they can easily recanalize after embolization (Salis *et al.* 2015). In order to effectively solve these problems, we used tissue engineering technology to introduce a "live cell" component to these embolic materials, namely we prepared a tissue-engineered embolic material, and introduced this aterial into the malformed vascular lumen of porcine subjects using a microcatheter technique allowing it to regenerate into an "autologous living tissue" with a predetermined mechanical strength, thereby permanently occluding the deformed blood vessels.

This study presents preliminarily data supporting the application of C/GP and fibroblasts in the treatment of cAVMs using rete mirabile (REM) as a model. We evaluated the pathological changes in the REM tissue of these porcine models 6 weeks after embolization and provided sufficient evidence to suggest that this may be a novel liquid embolic material for the endovascular treatment of cAVM.

MATERIALS AND METHODS

Establishment of the fibroblast bank

Fibroblasts were obtained from pig skin via enzymatic digestion and the fibroblast bank was established

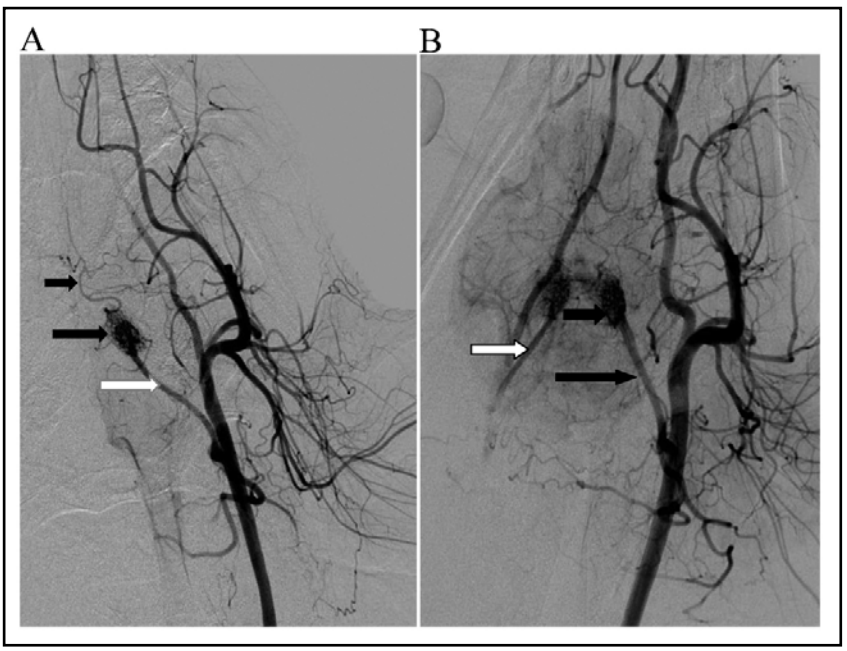

Fig. 1. Modeling of cAVM. A: Group L was not performed common carotid artery angiography, so it can only be seen the pharyngeal ascending artery (white arrow) emits the REM (long black arrow), and the REM re-aggregates into the internal carotid artery (short black arrow) in the brain; B: The CVA angiography of the experimental group shows that the cAVM model of pig was successfully established. The blood supply artery is the pharyngeal ascending artery of one side (long black arrow), the deformed vascular group is the skull base microvascular network (short black arrow), and the drainage vein is the carotid artery and the internal jugular vein anastomosis (white arrow) after microscopic anastomosis. cAVM: cerebral arteriovenous malformation; REM: rete mirabile; CVA: coronary venous angiography.

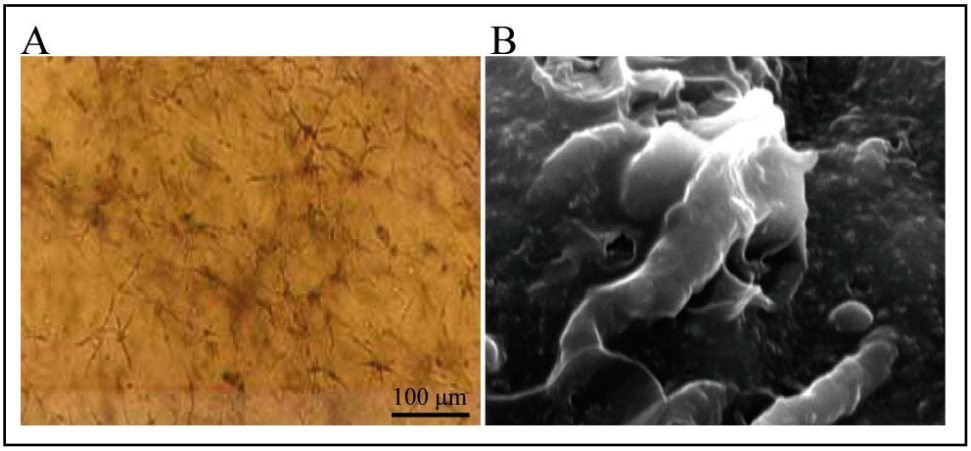

Fig. 2. The fibroblasts cultured for 21 days in the C/GP gel A: light microscopy (×100); B: electron microscopy (×5000). C/GP: chitosan/β-glycerophosphate sodium.

using *in vitro* culture, passage, cryopreservation and resuscitation techniques. After trypsin digestion, the epidermis was removed and the dermis was transferred to a culture dish, this dish was then covered with 0.25% trypsin and the digestion was stopped by adding 2 mL of Dulbecco's modified Eagle medium (DMEM) after visible cytoplasm retractation which caused the cells to become round and the cell gap to increase.

Evaluating fibroblast-alginate gel complex compatibility

The fibroblasts from the fibroblast bank were then resuscitated, cultured, trypsinized and diluted to prepare various cell suspensions. These suspensions were mixed with aqueous C/GP solution at room temperature and allowed to rapidly solidify at 37 °C to create the fibroblast-C/GP gel complexes. These complexes were translucent, colorless and solid.

These complexes were suspended and cultured in DMEM supplemented with 10% of newborn calf serum and the cytocompatibility of the fibroblast-C/GP gels were determined by regularly evaluating the adhesion, migration, aggregation and proliferation of the fibroblast-C/GP gel using light and scanning electron microscopy. The optimal growth conditions of these complexes were then determined, as well as the optimal ratio of cell/C/GP gel, allowing us to achieve a dynamic balance between C/GP degradation and cell growth.

Animal preparation

We selected domestic pigs as our animal model and used a total of 26 pigs for this study. These animals were both male and female, 25-30 kg in weight, 2-3 months old, light/dark cycle (12L:12D) and free access to food and water. After fasting for 12 hours before surgery, each pig was intramuscularly injected with 0.5 mg of atropine hydrochloride and 8 million units of penicillin sodium 30 min before surgery, and then treated with an intramuscular injection of ketamine hydrochloride 5 mg/kg and Sumianxin II 0.3 ml/kg to induce anesthesia. After the pigs lost consciousness and their eyelash reflex disappeared they were treated with a l% ketamine hydrochloride solution via intravenous injection with the flow rate under constant observation to allow for changes in the operative environment. A single multi-channel physiological recorder was used to monitor certain vital signs, including blood pressure, heart rate, and respiration during surgery. This study was carried out in strict accordance with the recommendations set out in the Guide for the Care and Use of Laboratory Animals from the National Institutes of Health. The animal use protocol was reviewed and approved by the Institutional Animal Care and Use Committee (IACUC) at Beihua University.

cAVM modeling

REM was set in the deformed vascular group and the pigs were divided into low-flow group (L) and high-flow group (H). In low-flow group (L), we employed the natural REM model, without microvascular anastomosis (Figure 1A). In high-flow group (H), one pharyngeal ascending artery was used as the blood supply artery and used to microscopically match the distal end of the contralateral common carotid artery and the proximal end of the internal jugular vein via microsurgical techniques so as to change the direction of blood flow. Allowing for the angiography of one side of the common carotid artery to represent the whole blood flow pathway (from one side of the ascending pharyngeal artery (AP), to the REM, to the AP of the anastomotic side, to the common carotid artery (CCA), to the anastomosis, and finally to the internal jugular vein (IJV) (Figure 1B).

Preparation of C/GP

To prepare the 2% (w/v) chitosan and 56% (w/v) β-glycerophosphate sodium 0.1M diluted hydrochloric acid solutions: l mL of concentrated hydrochloric acid (38%), containing 0.012 mol hydrochloric acid was diluted to 120 mL using triple-distilled water (this solution should be newly prepared and ready-to-use in each new preparation); then 5 g of chitosan was dissolved in this 0.1M hydrochloric acid and stirred at room temperature to produce a 250 mL solution that

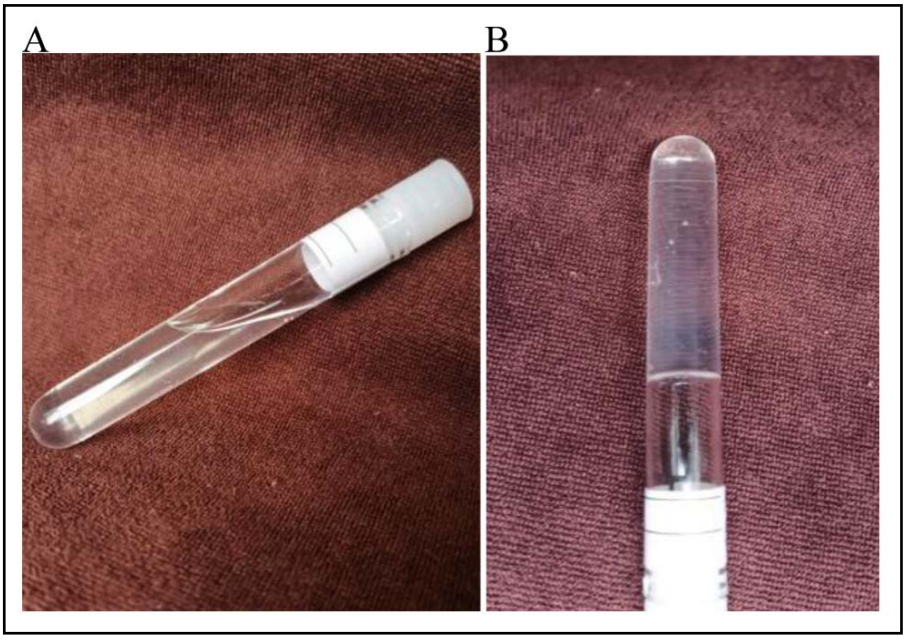

Fig. 3. The gelation test of 7:1 C/GP solution (A: the C/GP material is liquid at less than 37 °C; B: The C/GP material is gel at 37 °C). C/GP: chitosan/β-glycerophosphate sodium.

was autoclaved at 121 °C for 20 min and stored at 4 °C for future use. Then 28 g of β-glycerophosphate sodium was used to prepare a 56% (w/v) β-glycerophosphate solution in 50 mL of triple-distilled water. This was then filter sterilized and autoclaved at 121 °C for 20 min and stored at 4 °C for future use.

Intraoperative procedure for C/GP embolization of the REM

The femoral artery below the depression between the femoral muscle and the pubis muscle was first punctured using an indwelled 6F catheter sheath, with the Y and T valves connecting to the perfusion system. Heparin sodium 70U/KG was then pumped through the perfusion system and the 5F contrast catheter was selectively inserted into one side of the CCA in the L group or the CCA contralateral side in the H group. This was then followed by digital subtraction angiographic (DSA) examination using an Ultravist 300 and a high pressure syringe (injection flow rate was 4 ml/s, and the dose as 7 ml) which was used to evaluate the basic condition of the AP, REM and other connected arteries. A 6F flat guide catheter was then used to reach the REM end proximal to the AP. One microcatheter was then selectively inserted into the REM using the pharyngeal artery and a guiding catheter. After the animals were treated with a bolus-injection of contrast agent and the DSA evaluations were complete the C/GP solution was injected through the microcatheter (injection flow rate as 0.2 ml - 0.5 ml/min, injection dose was 0.5-1.0 ml and injection time was 1.5-5 min). In order to observe the degree of embolization, we timed the onset of "smoking" (which revealed the embolization and flow of the contrast agent) following injection and then the contrast agent was reintroduced and DSA examination was completed a second time. If the REM was not completely occluded, the embolic agent was continuously injected until the REM was confirmed to be completely embolized. After the embolization treatment was completed the microcatheter was slowly withdrawn and the angiographic examinations were performed at 2 and 6 weeks post-surgery, with these evaluations serving to demonstrate any recanalization of the blood vessels.

Treatment after embolization

The animals were killed using intravenous injection of a lethal dose of pentobarbital after angiography six weeks after embolization. The brain tissues, including the REM were then completely removed fixed in 10% formalin, exposed to routine dehydration and embedded in paraffin. These samples were then sectioned and subjected to H&E staining for histological examination.

Statistical method

Group differences were considered statistically significant at $p < 0.05$, as assessed by Student's t-test, one-way analysis of variance (ANOVA) followed by Fisher's least significant difference post hoc test using Origin 2017 (OriginLab Corporation).

RESULTS

The fibroblasts cultured for 21 days in the C/GP gel (seeding density as 1.0×10^6 /ml) exhibited denser tissue structures (Figure 2A) and a more pronounced star-like appearance (Figure 2B).

The average gelation time for the 7:1 C/GP solution at 37 °C was 120 seconds when 1 g of strontium powder or 1 mL of chloropyrene per 10 ml of the C/GP solution was added as the developer (Figure 3).

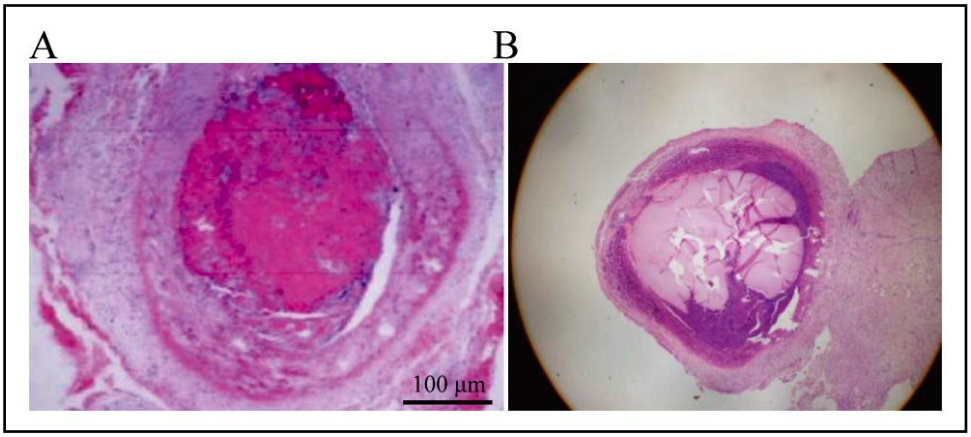

Fig. 4. Histological examination of microvascular network (A: REM in the skull base microvascular network. The REM vessels have the intima and adventitia, and there is scattered connective tissue between the microvessels with a transverse diameter as 80-320 μm; B: After 6 weeks of REM embolization, the C/GP gel fills the REM vascular lumen, the fibrous tissue grows inside, the membrane is intact, and there is no obvious inflammatory response). REM: rete mirabile; C/GP: chitosan/β-glycerophosphate sodium.

All 13 pigs in group L survived the surgery with no infections in the incision or limb hemiplegia. Only 12 of the pigs in group H survived surgery with one animal dying from spasm and respiratory depression during embolism. The REM and external carotid artery were embolized during surgery and one animal presented with lateral paralysis, masticatory muscle weakness and weight loss.

Histological examinations

Results of the histological examinations before REM embolization (Figure 4A) show that the diameter of the REM blood vessels were between 80 and 320 μm, which was very close to the diameter of the AVM blood vessels found in the human brain. The microvessels were arranged in a mutually intersecting manner and were morphologically similar to the abnormal vascular masses found in human brain arteriovenous malformations. The histological results for REM 6 weeks post embolization demonstrated that the C/GP gel filled the lumen of the REM, the fibroblasts were able to proliferate, the intima was intact and there were no obvious inflammatory reactions (Figure 4B).

Angiography

Angiography of the DSA before embolization: The pharyngeal ascending arteries in all 26 pigs were derived from the common carotid artery and these pharyngeal ascending arteries sent out terminal branches which formed REM within the cavernous sinus. The REM was shown to reaggregate with the internal carotid artery in the brain and supplied brain tissue in the intracranial branch. In addition, the two external anastomoses of the pig's external carotid artery (ramusanastomoticus RA) and the anastomotic artery (arteriaanastomotica AA) were also shown to participate in the REM blood supply (Figure 5A, B).

Angiography at Weeks 2 and 6 after embolization: the REM in eight out of the 12 pigs in the L group remained completely undeveloped (Figure 5E, F) and although the pharyngeal ascending artery in four animals were shown to be embolized, RA was still seen in the later

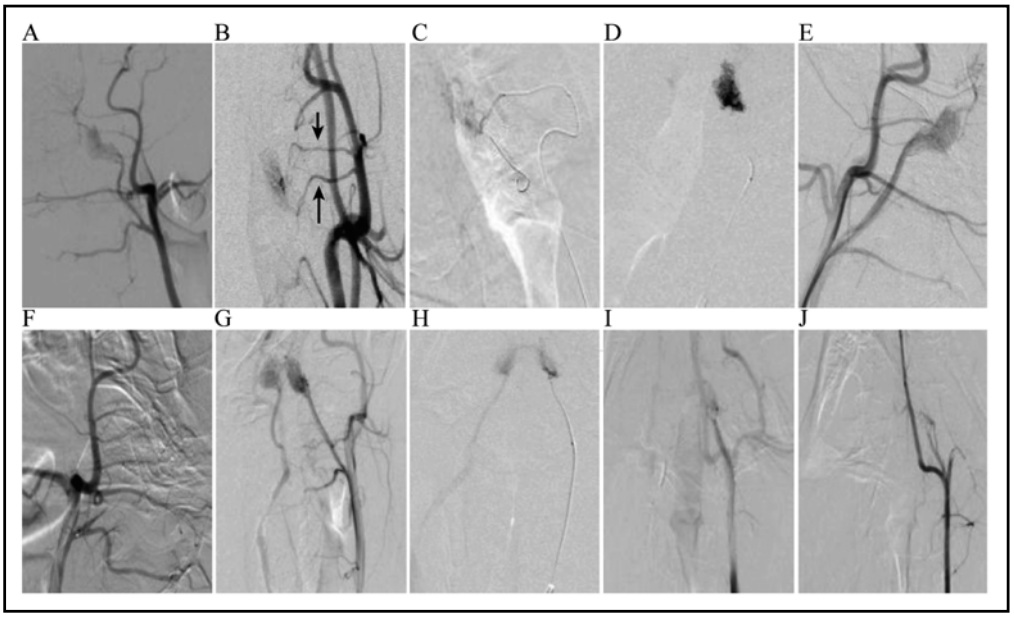

Fig. 5. Angiography of DSA (A: Unilateral REM; B: Angiographic images of Unilateral REM, AA short arrow, RA long arrow; C: RA ultra-selective angiography; D: RA after embolization; E: Before embolization; F: After embolization; G: Before embolization; H: Ultra-selective angiography before embolization; I: Bilateral REM don't develop after embolization; J: Bilateral REM don't develop after. Embolization). DSA: digital subtraction angiographic; REM: rete mirabile; AA: arteria anastomotica; RA: ramus anastomoticus.

parts of the REM, namely the pharyngeal ascending artery was embolized while the AA continued to supply blood to the REM. After the microcatheter super selectively entered the RA (Figure 5C) and the AA was re-embolized we were able to demonstrate that the REM was completely embolized (Figure 5D). The 12 pigs in group H all demonstrated the successful production of a cAVM phenotype prior to embolization (Figure 5G, H). The bilateral REM was not developed following C/GP embolization (Figures 5I, J) and angiography at 6 weeks post-surgery revealed no recanalization.

Intraoperative characterization

During the administration of the embolic agent we injected an additional bolus and noted that there was no resistance within the microcatheter. Combined with the ease of administration, the ability to control the time (1.5-3 min) and the total dose (0.5-1.0 mL) we suggest that this is a viable clinical intervention for cAVM. When the microcatheter was withdrawn after embolization, there was no adhesion between the end of the microcatheter and the embolic agent.

Histological examination after embolization

General observation revealed that the structures in the bilateral pharyngeal ascending arteries, REM and internal carotid artery were consistent with the initial DSA evaluations. There were no abnormalities in the brain tissues from group L, and the REM embolization was complete on the embolization side. The REM on the embolized side was harder and paler than on the contralateral side while the embolic material remained jelly-like. The REM was easily peeled from the rupture hole in the base of the skull. The two sides of the REM in group H were harder and paler, and the embolic material remained jelly-like.

Light microscopy showed that the gel in the lumen of the REM specimens was evenly dispersed, indicating that the vascular cavity was completely embolized and the hydrogel remained inside the lumen of these vessels. There was no inflammatory reaction around the blood vessels, the smooth muscle layer was intact, the intima of the vessel walls was clearly visible and there was also no exfoliation or necrosis in the vessel walls. (Figure 4B).

DISCUSSION

Arteriovenous malformation (AVM) is a common form of congenital cerebral vascular dysplasia (Zhang *et al.* 2016). The arteries and veins are directly connected without the intervention of capillaries, resulting in a series of hemodynamic disorders. It's common in young adults aged between 20 and 40 years old and the main clinical manifestations include recurrent intracranial hemorrhage, epilepsy, headache and neurological deficits (Osbun *et al.* 2017; and Tranvinh *et al.* 2017). The annual incidence of cerebral hemorrhage is between 2 and 3%, and the mortality rate is around 1-2% (Gabriel *et al.* 2010; Kim *et al.* 2009).

At present, there are several representative embolic materials commonly used in China and abroad including adhesive liquid embolic materials and non-adhesive liquid embolic materials. n-Butyl cyanide propionate (NBCA) is the most common of the adhesive liquid materials (Starke *et al.* 2009) and in 2000, the US Food and Drug Administration (US FDA) approved NBCA for use in endovascular embolization. NBCA liquid glue has a low viscosity before gelation and a short gelation time (commonly known as the three-second glue), which is not conducive to the fine manipulation of this material during injection. This attribute may increase the probability of entering a dangerous anastomosis which may lead to intracranial hemorrhage. NBCA also becomes harder after entering its gel form in the body which can complicate surgical resection after embolization. Moreover, this embolic agent can adhere to the polymer materials of the microcatheter and block its openings resulting in the microcatheter may be stuck in the skull. Currently the only non-adhesive liquid embolic material in use is ONYX gel which has also received FDA approval for use in the treatment of cAVM. ONYX gel is comprised of a mixture of vinyl alcohol copolymer (EVOH), dimethyl sulfoxide (DMSO) and strontium powder (Singfer *et al.* 2017), but since DMSO is an organic solvent with proven vascular toxicity, this formulation is less than ideal (Bakar *et al.* 2010). Onyx gel precipitates in blood vessels and forms a sponge-like solid, and when the diseased tissue is surgically resected after embolization, it is softer than NBCA gel and resection results in less bleeding (van Rooij *et al.* 2012). Onyx gel can induce a mild inflammatory response in the vessel walls but because it is non-adhesive, it can be injected over a long time ensuring more complete embolization without resulting in tube-sticking or blockage. Due to the addition of the developer powder, Onyx gel is clearly visible throughout the embolization process (Vollherbst *et al.* 2022) and can be used to treat both low-flow and high-flow cAVM lesions (Wang *et al.* 2015). However, Onyx gel needs a specific microcatheter that is resistant to DMSO and these parts tend to be more rigid which is further complicated by the fact that the microcatheter needs to be close to the site of the lesion (Vollherbst *et al.* 2017) In addition, if the injection rate is too fast, DMSO can exert a toxic effect of the blood vessel walls which may result in vascular endothelial cell necrosis and severe vasospasm (Van *et al.* 2021).

Liquid embolic materials with non-stick properties and no organic solvent supplementation would be an ideal solution, and given the fact that hydrogels are known to meet these criteria it is obvious that they should be evaluated in these types of applications (Poursaid *et al.* 2016). Hydrogels are a distinct class of polymer that swells when they absorb water and can retain a large volume amount of water without

dissolving. Because their properties are very similar to those of the body tissues, they have been shown to induce less irritation in surrounding tissues and have good histocompatibility (Shimohira *et al.* 2018). However, several of the well-known hydrogels remain liquid at high temperatures and solidify at low temperatures making their administration to the aneurysm cavity complicated and may increase the risk of complications such as ectopic embolization due to material liquefaction. In 2000, Chenite *et al.* (2000) were the first to described the use and preparation of a chitosan/β-glycerophosphate (C/GP) aqueous solution gel system as a novel injectable scaffold. This solution retains a physiological pH, is liquid at room temperature and can encapsulate both live cells and therapeutic proteins. This solution gels at body temperature and when it's administered to the body, it forms a biodegradable gel at the site of injection (Agarwal *et al.* 2013).

Wang *et al.* (2011) were first to use a thermosensitive chitosan/β-glycerol phosphate solution for embolization and were able to effectively embolize rabbit renal arteries with fairly reproducible results. There were no ectopic embolization, reduced tube sticking and catheter obstructions and there were fewer adverse events and changes during the embolization process. These animals also presented with improved postoperative condition and there were no special complications. Postoperative angiography also revealed no recanalization.

Here we used chitosan with the following specifications: viscosity 130 mPa.s, molecular weight 8.04 million Daltons and 90% deacetylation. Chitosan and β-glycerophosphate sodium can be mixed in varying proportions here we used a ratio of 7:1, which produced a pH value of 7.28, a mechanical strength of up to 14 kPa and an increased cell survival rate (89.0±2.7%). These parameters suggest that this solution has the potential to be a safe and effective liquid embolic material, which is supported by several previously reported *in vitro* and small animal experiments (Foley *et al.* 2016; Han *et al.* 2014). The average time required for gelation of the 7:1 C/GP solution at 37 °C is 120 seconds and 1 g of strontium powder or 1 mL of chloropyrene is sufficient to develop up to 10 mL of the C/GP solution.

Toxicity and pathological results

Chitosan has several good characteristics lending it credibility as an embolic material these include a high degree of biocompatibility, known antibacterial/antimicrobial/antiviral activity, demonstrated anticancer activity and being biodegradable. These characteristics have all contributed to itsapproval by the FDA for use as a wound dressing (Patrulea *et al.* 2015). Sodium glycerophosphate is an organic compound found in the human body in its natural form and has been approved by the FDA for intravenous therapy. *In vitro* and *in vivo* evaluations have demonstrated the biocompatibility of C/GP (Deng *et al.* 2017) and histological examination after embolization revealed no abnormalities in the treated brain tissues. Light microscopy showed that the REM lumen was filled with the gel material, the intima of the walls was clearly visible and the smooth muscle layer was intact. No exfoliation and necrosis of the vessel walls was observed and there was no inflammatory reaction around the blood vessels, indicating that C/GP has no toxic effect on blood vessels (Zhou *et al.* 2015). C/GP was developed well after the developer was added to the powder, but in the histological sections, the metal tantalum powder did inhibit sectioning, but liquid developers, including chloropyrene, had no impact on the sectioning of the histology specimens.

Precautions during embolization

The injection rate of C/GP should be carefully calibrated and the bolus flow rate should be monitored. If the flow rate is too high the C/GP will not form its hydrogel at the site of the cAVM and may enter the drainage vessels damaging the blood flow to the brain. If the flow rate is too slow, it will cause premature precipitation of the hydrogel, resulting in C/GP gelation in the catheter and catheter blockage. Here we successfully used a bolus flow rate of 0.2 ml-0.5 ml/min and a dose of 0.5-1.0 ml with an injection time of 1.5-5 min.

Study limitations: Both male and female pigs were used, which may create additional confound of sex in the study.

CONCLUSION

Our results showed that the pathological changes in the REM tissue of these porcine models 6 weeks after embolization and provided sufficient evidence to suggest that this may be a novel liquid embolic material for the endovascular treatment of cAVM. C/GP and fibroblasts can be used in the embolization of cAVM and that this approach may have broad application an ideal embolization material for the treatment of cAVM.

ACKNOWLEDGEMENTS

This study was supported by the research Projects of Jilin Provincial Health and Family Planning (Project), 2014ZC055; "Twelfth Five-Year" Science and Technology Research Projects of Jilin Provincial Education Department, 2015150.

CONFLICTS OF INTEREST

The authors declare no conflict of interest.

REFERENCES

1 Breitsamer, M., Winter, G. (2019). Vesicular phospholipid gels as drug delivery systems for small molecular weight drugs, peptides and proteins: State of the art review. Int J Pharm. **557**: 1–8.
2 Bakar B, Oruckaptan HH, Hazer BD, Saatci I, Atilla P, Kilic K, et al. (2010). Evaluation of the toxicity of onyx compared with n-butyl 2-cyanoacrylate in the subarachnoid space of a rabbit model: An experimental research. Neuroradiology. **52**: 125–134.
3 Chen, C. J., Ding, D., Derdeyn, C. P., Lanzino, G., Friedlander, R. M., Southerland, et al. (2020). Brain arteriovenous malformations: A review of natural history, pathobiology, and interventions. Neurology. **95**: 917–927.
4 Chen QY, Zhu XR, Zhang Y (2017). The Hemodynamic Changes in Patients with Cerebral Arteriovenous Malformations before and after Interventional Embolization Therapy with Glubran 2 Acrylic Glue. Eur Neurol. **78**: 169–175.
5 Chenite A, Chaput C, Wang D, Combes C, Buschmann MD, Hoemann CD, et al. (2000). Novel injectable neutral solutions of chitosan form biodegradable gels in situ. Biomaterials. **21**: 2155–2161.
6 Deng A, Kang X, Zhang J, Yang Y, Yang S (2017). Enhanced gelation of chitosan/β-sodium glycerophosphate thermosensitive hydrogel with sodium bicarbonate and biocompatibility evaluated. Mater Sci Eng C Mater Biol Appl. **78**: 1147–1154.
7 Foley PL, Ulery BD, Kan HM, Burks MV, Cui Z, Wu Q, et al. (2016). A chitosan thermogel for delivery of ropivacaine in regional musculoskeletal anesthesia. Biomaterials. **34**: 2539–2546.
8 Gabriel RA, Kim H, Sidney S, McCulloch CE, Singh V, Johnston SC, et al. (2010). Ten-year detection rate of brain arteriovenous malformations in a large, multiethnic, defined population. Stroke. **41**: 21–2
9 van der Kamp, L. T., Rinkel, G. J. E., Verbaan, D., van den Berg, R., Vandertop, W. P., Murayama, Y., et al. (2021). Risk of Rupture After Intracranial Aneurysm Growth. JAMA neurology. **78**: 1228–35.
10 Gross BA, Moon K, Mcdougall CG (2017). Endovascular management of arteriovenous malformations. Handb Clin Neurol. **143**: 59–68.
11 Han HD, Nam DE, Seo DH, Kim TW, Shin BC, Choi HS (2014). Preparation and biodegradation of thermosensitive chitosan hydrogel as a function of pH and temperature. Macromol Res. 12: 507-511.
12 Jabbour MN, Elder JB, Samuelson CG, Khashabi S, Hofman FM, Giannotta SL, et al. (2009). Aberrant angiogenic characteristics of human brain arteriovenous malformation endothelial cells. Neurosurgery. **64**: 139–146.
13 Kim H, Pawlikowska L, Chen Y, Su H, Yang GY, Young WL (2009). Brain arteriovenous malformation biology relevant to hemorrhage and implication for therapeutic development. Stroke. **40**: S95–S97.
14 Lopes DK, Moftakhar R, Straus D, Munich SA, Chaus F, Kaszuba MC (2016). Arteriovenous malformation embocure score: AVMES. J Neurointerv Surg. **8**: 685–691.
15 Massoud TF, Vinters HV, Chao KH, Viñuela F, Jahan R (2000). Histopathologic characteristics of a chronic arteriovenous malformation in a swine model: preliminary study. AJNR Am J Neuroradiol. **21**: 1268–1276.
16 Murayama Y, Viñuela F, Ulhoa A, Akiba Y, Duckwiler GR, Gobin YP, et al. (1998). Nonadhesive liquid embolic agent for cerebral arteriovenous malformations: preliminary histopathological studies in swine rete mirabile. Neurosurgery. **43**: 1164–1175.
17 Ning X, Zhao C, Pang J, Ding Z, Wang Y, Xu K, et al. (2015). Experimental study of temperature-sensitive chitosan/β-glycerophosphate embolic material in embolizing the basicranial rete mirabile in swines. Exp Ther Med. **10**: 316–322.
18 Osbun JW, Reynolds MR, Barrow DL (2017). Arteriovenous malformations: epidemiology, clinical presentation, and diagnostic evaluation. Handb Clin Neurol. **143**: 25–29.
19 Patrulea V, Ostafe V, Borchard G, Jordan O (2015). Chitosan as a starting material for wound healing applications. Eur J Pharm Biopharm. **97**: 417–426.
20 Poursaid A, Jensen MM, Huo E, Ghandehari H (2016). Polymeric materials for embolic and chemoembolic applications. J Control Release. **240**: 414–433.
21 Salis A, Rassu G, Budai-Szűcs M, Benzoni I, Csányi E, Berkó S, et al. (2015). Development of thermosensitive chitosan/glicerophospate injectable in situ gelling solutions for potential application in intraoperative fluorescence imaging and local therapy of hepatocellular carcinoma: a preliminary study. Expert Opin Drug Deliv. **12**: 1583–1596.
22 Shimohira M, Kawai T, Hashizume T, Muto M, Kitase M, Shibamoto Y (2018). Usefulness of Hydrogel-Coated Coils in Embolization of Pulmonary Arteriovenous Malformations. Cardiovasc Intervent Radiol. **41**: 848–855.
23 Singfer U, Hemelsoet D, Vanlangenhove P, Martens F, Verbeke L, Van Roost D, et al. (2017). Unruptured Brain Arteriovenous Malformations: Primary ONYX Embolization in ARUBA (A Randomized Trial of Unruptured Brain Arteriovenous Malformations)-Eligible Patients. Stroke. **48**: 3393–3396.
24 Starke RM, Komotar RJ, Otten ML, Hahn DK, Fischer LE, Hwang BY, et al. (2009). Adjuvant embolization with N-butyl cyanoacrylate in the treatment of cerebral arteriovenous malformations: outcomes, complications, and predictors of neurologic deficits. Stroke. **40**: 2783–2790.
25 Tranvinh E, Heit JJ, Hacein-Bey L, Provenzale J, Wintermark M (2017). Contemporary Imaging of Cerebral Arteriovenous Malformations. AJR Am J Roentgenol. **208**: 1320–1330.
26 van Rooij WJ, Jacobs S, Sluzewski M, van der Pol B, Beute GN, Sprengers ME (2012). Curative embolization of brain arteriovenous malformations with onyx: patient selection, embolization technique, and results. AJNR Am J Neuroradiol. **33**: 1299–1304.
27 Vollherbst, D. F., Chapot, R., Bendszus, M., Möhlenbruch, M. A. (2022). Glue, Onyx, Squid or PHIL? Liquid Embolic Agents for the Embolization of Cerebral Arteriovenous Malformations and Dural Arteriovenous Fistulas. Clin Neuroradiol. **32**: 25–38.
28 Vollherbst DF, Sommer CM, Ulfert C, Pfaff J, Bendszus M, Möhlenbruch MA (2017). Liquid Embolic Agents for Endovascular Embolization: Evaluation of an Established (Onyx) and a Novel (PHIL) Embolic Agent in an In Vitro AVM Model. AJNR Am J Neuroradiol. **38**: 1377–1382.
29 Wang Q, Quan Z, Li Z (2015). Endovascular Treatment of Two High-Flow Brain Arteriovenous Fistulas with a Combination of Detachable Coils and Onyx in an Infant: Case Report and Review of Literature. Pediatr Neurosurg. **50**: 216–219.
30 Wang Y, Xu N, Luo Q, Li Y, Sun L, Wang H, et al. (2011). In vivo assessment of chitosan/β-glycerophosphate as a new liquid embolic agent. Interv Neuroradiol. **17**: 87–92.
31 Zhang R, Zhu W, Su H (2016). Vascular Integrity in the Pathogenesis of Brain Arteriovenous Malformation. Acta Neurochir Suppl. **121**: 29–35.
32 Zhou HY, Jiang LJ, Cao PP, Li JB, Chen XG (2015). Glycerophosphate-based chitosan thermosensitive hydrogels and their biomedical applications. Carbohydr Polym. **117**: 524–536.